

POSTDICTION OF STRONG MOTION FOR THE 1923 KANTO EARTHQUAKE CONSIDERING ITS HETEROGENEOUS SOURCE PROCESS

Y SHIBA¹, T ANNAKA² And M SHIMADA³

SUMMARY

The ground motion in a short-period range of the 1923 Kanto earthquake was estimated by the stochastic Green's function method, which is based on the empirical Green's function method but uses the artificial seismogram as the element event. A variable-slip distribution on the main shock fault is also considered. The artificial ground motion substituted for the observed one is calculated from the theoretical source spectrum and the empirical path and site effect. For the source model of the 1923 Kanto earthquake, we assumed the slip distribution to have two independent asperities, following Wald and Somerville (1995). To describe a heterogeneous rupture process for the semi-empirical method, two models that have different filter functions were proposed. In the first model amplitude of the filter function at each subfault is assumed to be proportional to the slip value. This means the rise time has a fixed value over the whole fault plane. In the second model the filter function is represented as a linear summation of waves radiated from the asperities and whole fault, both of which obey the ω^{-2} model independently. This model takes account of the stopping phase on the periphery of the asperity as well as the entire fault, therefore the high-frequency waves are expected to be radiated more strongly. We call the first method "the proportion method", and second "the superposition method" in this paper. As a result the superposition method generates remarkably larger short-period ground motions than the conventional method, which uses a source model with uniform slip, whereas the proportion method shows relatively similar amplitude to the conventional method in the range of the standard deviation estimated from the randomness of phase property.

INTRODUCTION

The 1923 Kanto earthquake ($M_{JMA}=7.9$) was one of the most damaged historic events in Kanto district, Japan. For earthquake resistant design and emergency plan at these area, precise estimation of the ground motions during the 1923 event is important in practical meaning. Although many researchers have studied about source mechanism of the 1923 event [e.g., Kanamori, 1971; Ando, 1974; Matsu'ura et al., 1980; Matsu'ura and Iwasaki, 1983], their results were so called macroscopic source model, which does not include a information of slip distribution. Recently, Wald and Somerville (1995) estimated spatial and temporal slip variations by a joint inversion combining geodetic and teleseismic data. By using this model, long-period [Sato et al., 1998] and short-period [Dan and Sato, 1999] ground motions were simulated taking account of a heterogeneous source process, especially effects of asperities.

For estimation of short-period seismic motion, the semi-empirical method [Hartzell, 1978; Irikura, 1986] has the advantage of eliminating heavy numerical computation and detailed modeling of propagating path and local site effect by utilizing small-event records as empirical Green's functions. When suitable observed records available for empirical Green's functions are not obtained, artificial small seismic motions calculated based on the theoretical source model (ω^{-2} model [Aki, 1967]) are substituted [Kamae et al., 1998]. Nowadays the method

¹ Earthquake Engineering Dept, Central Research Inst. Electric Power Industry, Abiko, Japan. cbar@criepi.denken.or.jp

² Tokyo Electric Power Services Co., Ltd., Tokyo, Japan Email: annaka@aed.tepsc.co.jp

³ Power Engineering R&D Center, Tokyo Electric Power Company, Kawasaki, Japan Email: t0594366@pmail.tepc.co.jp

mentioned above is named "the stochastic Green's function method" as modified scheme of the empirical Green's function method. Because the Green's function does not contain real path and local site effects in this method, we need to decide these effects from another information independently. However, a merit that the source effects from finite dimensions of fault plane can be considered is still remained. To apply the empirical or the stochastic Green's function method to a heterogeneous source process, which large earthquakes possess generally, the evaluation of the slip velocity function on the fault plane is one of the most important factors. Most of the variable slip models of actual large events are inverted from seismic data in the period of longer than 1 or 2 seconds, and the source time function (slip velocity function) is given as a smoothed one, like a triangle function. In order to apply the semi-empirical method for evaluation of the short-period ground motions based on the inverted source models like these, the slip velocity function must be extrapolated to the high frequency range, including the effects of heterogeneous slip distribution.

In this paper we propose the semi-empirical simulation scheme for large earthquakes with heterogeneous source process by modification to the filter functions, which approximately equal to the slip velocity function in the time domain. The basic formulation we employ is the stochastic Green's function method, and only horizontal S waves are evaluated. The site responses beneath the evaluation points are estimated empirically, by using recent seismic records observed at the site. Then we evaluate the strong motions for the 1923 Kanto earthquake at several points, using the variable slip model derived by Wald and Somerville (1995).

METHOD

Estimation of Site Response

The stochastic Green's function method needs an independent estimation of the propagating path and the local site effect. Since the frequency range of seismic waves of interest here is up to 10 or 20Hz, it is difficult to estimate these effects by the analytical approach using a subsurface velocity structure model, especially in case that evaluation points are located on a soft sedimentary basin. We adopted the empirical procedure based on observed seismic records for estimation of the site response in this study. As for the path effect, the Q_s values are given as $Q_s(f) = 100 f^{0.7}$ for $f > 1\text{Hz}$, and $Q_s=100$ (constant value) for $f < 1\text{Hz}$, following Sato (1990).

The site response from hard rock basement to surface is estimated by following procedure, under the condition that the strong motion records of the moderate earthquakes are stored at all evaluation points. The ground motions of the observed events are synthesized at the hypothetical hard rock basement, where the site amplification factor is assumed to be 2 in all analyzed frequency range. Here, we use the stochastic simulation algorithm [Boore, 1983] based on the ω^{-2} source model. Next, the Fourier spectral ratios from observed data to synthesized ones are taken, and the site response is obtained from the mean value of these. To reduce the fluctuation of the results, the stress parameters (stress drops in case of circular fault) of the analyzed events are also taken into consideration. Here, we estimate relative values of the stress parameters first, and determine the absolute value of at least one reference event. And finally, all stress parameters are obtained by multiplying both of them. The relative stress parameters are estimated by taking the spectral ratios from the reference event to another one. From the S wave spectral ratios, the relative stress parameters are derived as follows,

$$\begin{aligned} a'_0/a_0 &= CN \\ u'_0/u_0 &= Mo'/Mo = CN^3, \end{aligned} \tag{1}$$

where a'_0/a_0 and u'_0/u_0 are the spectral ratio in the high-frequency and the low-frequency part respectively, C denotes the stress parameter's ratio, and N is the scale parameter which is equivalent to the fault dimension's ratio from the reference event to another one.

Modeling of Heterogeneous Source Process Based on the Semi-empirical Method

The semi-empirical method for evaluating strong ground motions has been formulated as simulating the uniform slip rupture process on the fault area. Therefore, the summation scheme to synthesize waveforms of the target event from the element event is made under the restriction that both of the element and the target event obey the ω^{-2} scaling law. In order to extend this method to the variable-slip rupture process, various improvements have been made by many researchers. For example, Kamae and Irikura (1998) considered asperities located within the fault plane as independent subevents, and calculated the ground motions of the 1995 Hyogo-ken Nanbu earthquake ($M_{\text{JMA}}=7.2$) on the assumption that each subevent has a homogeneous rupture process. In their study the seismic moment is not preserved due to no slip outside asperities. Dan and Sato (1999) formulated the semi-

empirical scheme in the frequency domain. In their formulation the transform function for inference of the source spectrum consists of two corner frequencies, and one of them is equal to the ratio of the maximum slip velocity to the final slip on each subfault. They indicate both of them on subfaults are almost proportional to each other, so the difference of the transform functions between different subfaults are expected to be rather small but for the moment rate (amplitude).

We propose a new simulating method with the preservation of the seismic moment, or the averaged final slip. We begin with the basic procedure presented by Irikura (1986), which is formulated in the time domain. The ground motions from the target event are expressed as a superposition of seismic waves of the element events as follows,

$$U(t) = C \sum_{i=1}^N \sum_{j=1}^N \frac{r}{r_{ij}} F(t - t_{ij}) * u(t), \quad (2)$$

where $U(t)$ and $u(t)$ are the ground motion of the target and the element event respectively. The term r is the hypocentral distance of the element event and r_{ij} is that of the target event at the subfault of coordinates (i, j) . The terms C and N indicate the stress drop ratio and the scale parameter respectively, as written in equation (1). F is the filter function used for correction of the source time function, t_{ij} is the time shift calculated from the location of (i, j) -th subfault and the starting point of rupture. When the distribution of the slip is variable, the stress drop ratio C is also expected to show a spatial variation. We extend this formulation by replacing the constant factor C to the variable one C_{ij} according to the slip variation. For simplicity the static (averaged) stress drop of the target event is assumed to be equal to that of the element event. First of all, the fault plane of the target event is divided into the asperities and the outside of asperities, each of which has a constant slip value respectively. Next we assume that the asperity areas and the entire fault plane are represented as the ω^{-2} source model independently, and finally the seismic waves radiated from asperities and entire fault are calculated by the conventional semi-empirical method and they are superposed in the time domain. For the preservation of the total seismic moment, the slip values in the asperities are set to be the excess over the surrounding non-asperity area. In our formulation, the stress drop ratio outside the asperities, C_{OUT} is written as,

$$C_{OUT} = \frac{D_{OUT}}{d} \frac{1}{\sqrt{N_L N_W}} \approx \frac{D_{OUT}}{d} \frac{1}{N_T} \quad (3)$$

where D_{OUT} is the final slip outside the asperities, d is that of the element event, and N_L , N_W , N_T are the scale parameters for the fault length, width and the rise time, respectively. As for the inside of the asperity, C_{IN} is given by

$$C_{IN} = C_{OUT} + \frac{(D_{IN} - D_{OUT})}{d} \frac{1}{\sqrt{N_L^{IN} N_W^{IN}}} \approx C_{OUT} + \frac{(D_{IN} - D_{OUT})}{d} \frac{1}{N_T^{IN}}, \quad (4)$$

where D_{IN} , N_L^{IN} , N_W^{IN} and N_T^{IN} are the same factors as the equation (3), but are inside the asperity. We call our formulation as the superposition method hereafter. For the comparison with our method, we also evaluate the strong motions on the assumption that the stress drop ratio C_{ij} is simply proportional to the local slip value on the fault, which we call the proportion method. Figure 1 shows the filter function $F(t)$ multiplied by the stress drop ratio C_{ij} of these two methods and the conventional method. In the proportion method, the duration time of the

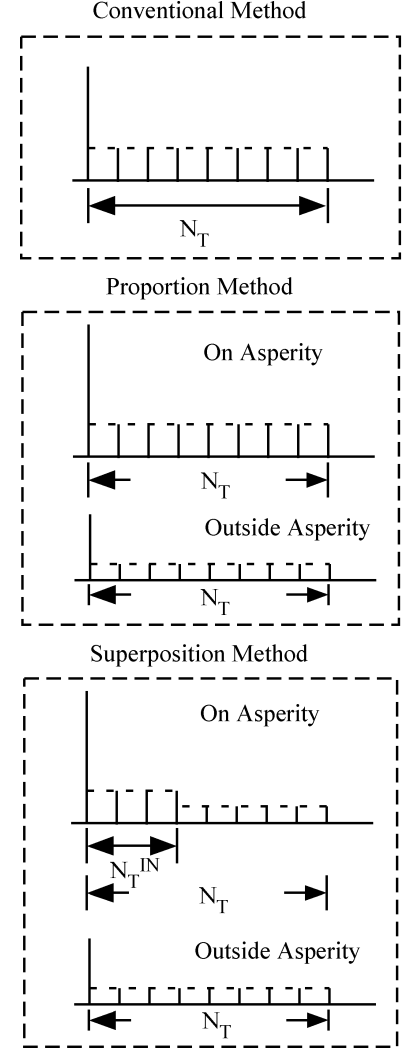


Figure 1: The filter function $F(t)$ multiplied by stress drop ratio C_{ij} for three different semi-empirical scheme

filter function, which means the rise time, is identical with that of the conventional method, and its spectral amplitude varies in the same way for all frequency range. The proportion method will yield similar results to the method developed by Dan and Sato (1999). Although their procedure allows the case that the slips and the slip velocities on the subfaults are not completely proportional to each other, they also indicate the proportional relation between the slips and the maximum slip velocities in the actual source process. As for the superposition method, the filter function on the asperity is represented as a linear summation of the contribution from the entire fault and that from the asperity itself, as shown in equation (4). Hence, in the superposition method the high-frequency seismic waves are excited more strongly from the asperity area, because the filter function holds the higher amplitude in the shorter duration time than that of other methods.

RESULTS

Site Responses of Evaluation Points Using Recent Observed Earthquakes

Figure 2 shows the location of the evaluation points and the epicenters of the recent events observed at more than one point. The fault area with two asperities of the 1923 event projected on the horizontal plane is also shown. The geometric position of the fault plane is based on Matsu'ura et al. (1980), and the distribution of the asperity is referred to Wald and Somerville (1995), which is discussed later. Four of the evaluation points, namely JZD, SAM, MSY and FUT from west to east, are located just on the fault plane. At all the evaluation points the strong ground motions have been observed since the 1980's or the beginning of the 1990's. The station JZD and TOG are located on the weathered rock, and other stations are on the soft sediment. At FUT there is a vertical seismometer array, so that we can utilize the records at rather rigid basement, where the S wave velocity is about 450m/sec. The magnitude of the observed events ranges from 2.9 to 6.7.

We chose the 1996 Yamanashi-ken Tobu earthquake ($M_{JMA}=5.3$) as the reference event to determine the absolute value of the stress parameter, because it was observed at the most evaluation points. The source spectra of the S waves are calculated from the records at bedrock stations near the epicenter of the

reference event, and the stress parameter is estimated by fitting to the Brune's source model [Brune, 1970, 1971]. Figure 3 shows the source spectra derived from the records at the bedrock stations and the best-fit theoretical spectrum. The site amplifications at the bedrock stations are fixed to 2 and the radiation coefficient is taken as 0.63 as the average value [Boore and Boatwright, 1984]. As a result, the stress parameter of the reference event is estimated to be 35MPa. For FUT and TOG, where the reference event was not observed, another relatively large event was selected as the reference event at each station and examined the same procedure. The estimated site responses at the evaluation points are shown in figure 4. The dotted lines indicate the standard deviations. To confirm the validity of our estimation, the ground motions are recalculated at the surface of the evaluation points by using the obtained site responses. Figure 5a shows the comparison of the peak ground accelerations of the synthesized waves with those of the observed ones. Figure 5b shows the case that the stress parameters of all analyzed events are set to be a constant value of 10MPa. These figures indicate the agreement between the synthesized peak acceleration and the observed one is improved obviously by the correction of the stress parameters.

Source Model of the 1923 Kanto Earthquake

Table 1 shows the macroscopic source parameters for the 1923 Kanto earthquake, following Matsu'ura et al. (1980) and Dan and Sato (1999). The fault plane of the 1923 event is divided into 10 subfault elements along the strike direction and 7 elements toward the dip direction. We put the two asperities near the starting point of the rupture and beneath the Miura Peninsula, following Wald and Somerville (1995). The slip values at the asperities are set to 7m and 8m respectively, as shown in figure 6. The rupture is assumed to start from the hypocenter and to propagate radially with a velocity of 3.0km/sec. Our fault model is slightly smaller than the original model of Wald and Somerville (1995), because we eliminate the low-slip subfaults at the periphery of the fault in their model. Furthermore, the rake angle on the subfault is variable in their model, but in our model it is assumed to be constant. Since the radiation pattern of the high-frequency seismic wave is smoothed due to the fluctuation of the rupture at the source and the scattering effect at the path [e.g., Liu and Helmberger, 1985]

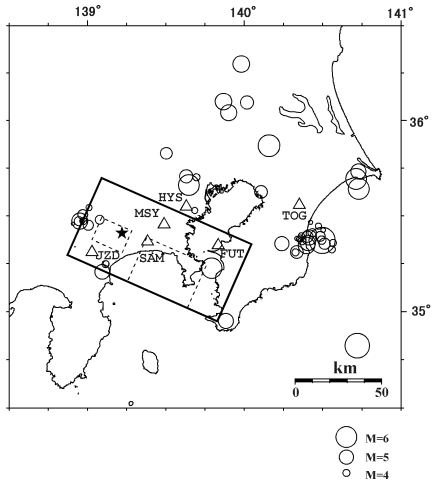


Figure 2: Location of the evaluation points (triangle), the epicenters of observed events (circle) and the fault of the 1923 Kanto earthquake projected on the horizontal plane (star indicates a nuclear point) with asperities (rectangular written in dotted line).

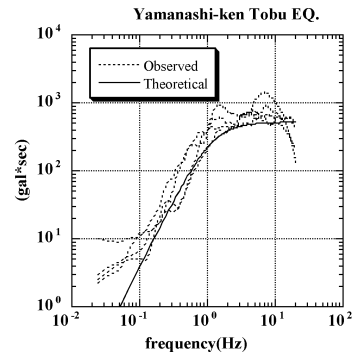


Figure 3: Source spectra derived from the records at the bedrock stations and the best-fit theoretical spectrum based on the ω^{-2} model

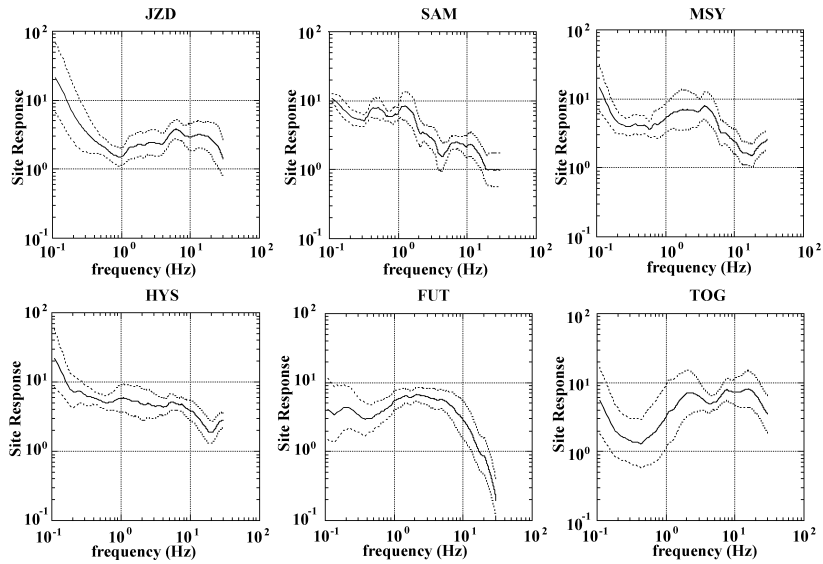


Figure 4: Estimated site responses at the evaluation points. The dotted lines show standard deviations.

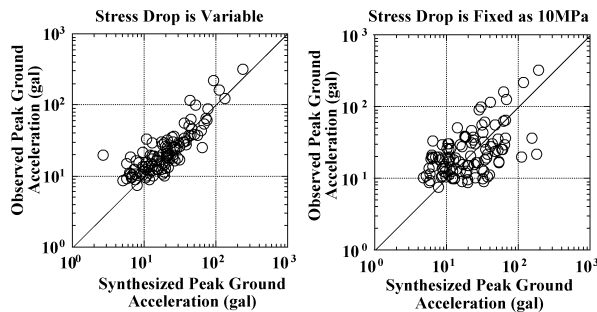


Figure 5a (left): Relationship between the peak ground accelerations of the synthesized waves and those of the observed ones
 Figure 5b (right): Same figure as 5a, but the case that stress parameters of synthesized events are set to be 10MPa

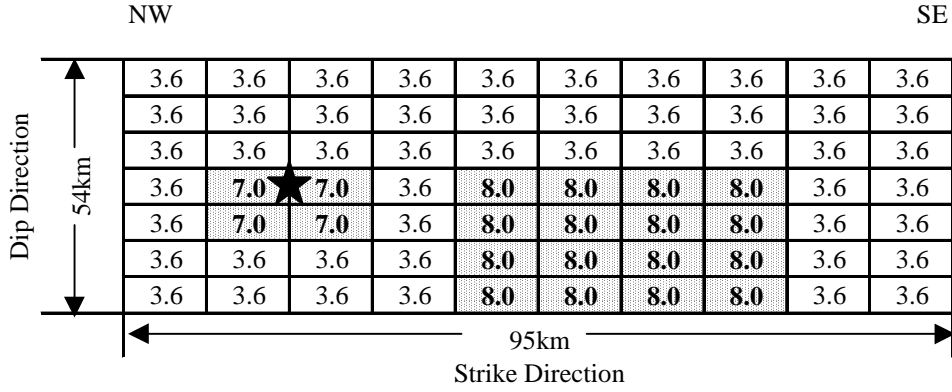


Figure 6: Slip distribution model of the 1923 event. The slip value is shown at each subfault in meters, and the star symbol indicates the starting point of rupture.

Table 1: Macroscopic source parameter of the 1923 Kanto earthquake

Latitude	35.41 N
Longitude	139.22 E
Depth	13.5 km
Seismic moment	8.37×10^{20} Nm
Density	2.8g/cm^3
S-wave Velocity	3.71 km/s
Strike	294°
Dip	25°
Rake	140°
Fault length	95 km
Fault width	54 km
Average slip	4.8 m
Stress drop	5.55 MPa

Table 2: Source parameters of the element event

Seismic moment	1.50×10^{18} Nm
Fault length	9.5 km
Fault width	7.7 km
Average slip	0.6 m
Stress drop	5.55 MPa

The ground motions of the element event were simulated by the Boore's method [Boore, 1983]. Table 2 shows the source parameters of the element event. The seismic moment of the element event equals the divided value of the total moment of the target event by the number of the subfaults, and the stress parameter (stress drop) is identical to the average value of the target event. In some evaluation points, the site responses at the lower frequency range are suppressed in order to avoid the unrealistic amplifications due to high noise level compared with signal (see figure 4). The duration time of T_d , which is assumed to be the function of only the magnitude in this study, is determined by the recursive way using the observed data, as following equation:

$$\log T_d = 0.30M - 0.314. \quad (5)$$

To level off the fluctuation of the waveforms due to the randomness of the phase property, ten seismic waves with different phases are calculated. Then, the ground motions of the 1923 event are synthesized by three different methods mentioned above. Figure 7a shows the examples of the simulated acceleration motions of the element event and the target event estimated by each method. The waveforms are band-pass filtered from 0.1 to 15 Hz. In figure 7a, the conventional method and the proportion method yield the comparably same levels of accelerations, whereas the superposition method shows about 1.5 times larger peak acceleration than others. The envelope shape of the wave train also become shorten in the superposition method, which suggests the concentration of the seismic energy in short duration. Figure 7b shows the acceleration response spectra obtained by averaging ten spectra derived from the synthesized waves of different phase properties. Figure 7b indicates the superposition method generates higher spectral amplitude in the period range shorter than 3 second. In figure 8 we show the distribution of the peak ground accelerations at each evaluation point. The order of the evaluation points in the x-axis is related to the location on the map from west to east. As shown in figure 8, the stations of MSY and SAM show the high peak values, especially the results by the superposition method exceed 1G. In the actual situation, the nonlinear response of the soft subsurface layer, which we do not take account of here, is expected to reduce the high-frequency amplitude. On the other hand relatively lower accelerations than

these two stations are simulated at JZD and FUT, though they are also located just on the fault. This is mainly due to the difference of the site conditions as seen in figure 4. At all the evaluation points the peak acceleration values obtained by the superposition method are obviously higher than those by other two methods, if the range of the error bar is taken into consideration.

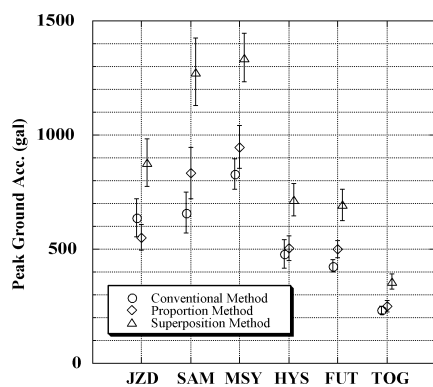
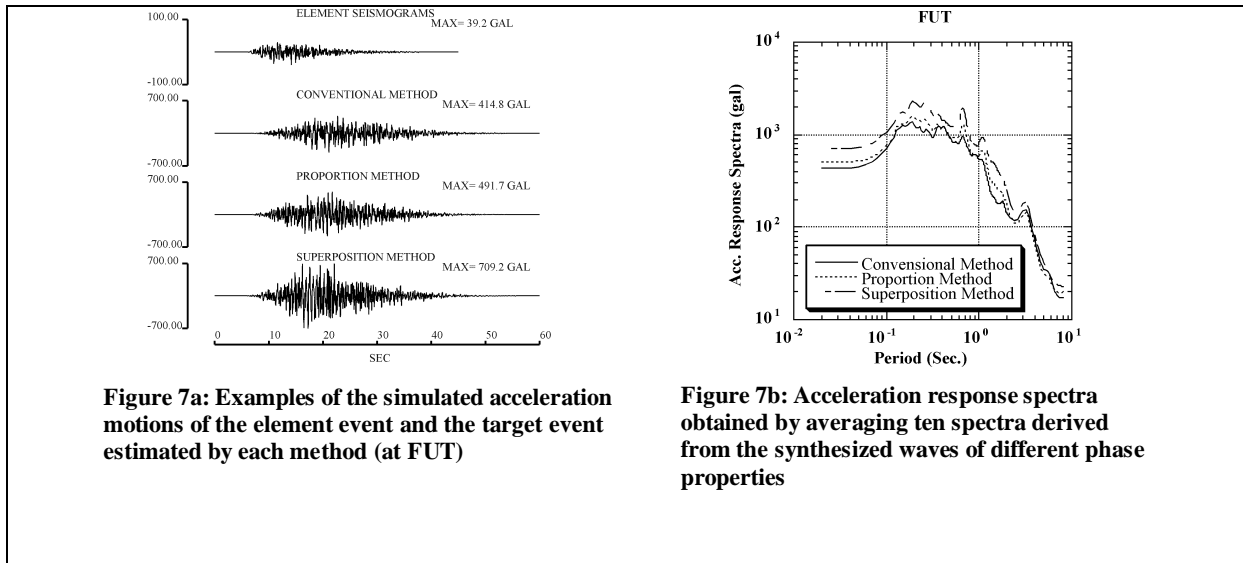


Figure 8: Distribution of the peak ground accelerations at the evaluation points

results in the formulation of the barrier model in a frame of the semi-empirical simulation. At the same time, the superposition method simulates the extreme condition for the high-frequency seismic radiation, because of an assumption that only the sudden change of slips occurs at periphery of asperities. The actual seismic source will allow the both of sudden change and smooth variation of the slip for the rupture process near the edge of asperities. Practically the superposition method produces the most severe seismic motions for buildings and instruments whose natural frequency is relatively high. Therefore the result of the superposition method is available for the input ground motion in seismic design for important structures as the upper limit of the high-frequency seismic waves for the roughly estimated source model.

DISCUSSION

The seismic source modeling for predicting or postdicting the high-frequency strong motions is essentially the spatial and temporal extrapolation of the rupture process, especially the slip velocity function, based on the physically reasonable assumption. The high-frequency waves are radiated from the point where the rupture velocity varies suddenly due to the change of the stress state on the fault [Bernard and Madariaga, 1984]. For a uniform rupture process, sudden change of the rupture velocity occurs at only the periphery of the fault itself, where the rupture stops entirely, and generates a "stopping phase" [Sato and Hirasawa, 1973; Madariaga, 1976]. In case of variable slip model, the periphery of an asperity will also excites high-frequency waves if the rupture velocity changes there. For the theoretical source modeling, the rupture process in this manner is corresponds to the "barrier model" in the narrow sense [Das and Aki, 1977]. The superposition method

CONCLUSIONS

We proposed the semi-empirical simulation scheme for large earthquakes with heterogeneous source process based on the stochastic Green's function method, and evaluated the strong motions for the 1923 Kanto earthquake, using the variable slip model derived by Wald and Somerville (1995). The site response beneath the evaluation point was estimated empirically, by using recent seismic records observed at the site. In our new formulation for simulating the variable slip rupture process, the fault plane is divided into the asperities and the outside of asperities, and the seismic waves radiated from the asperities and the entire fault are superposed in time domain. Both of them are assumed to satisfy the ω^{-2} scaling law independently, and the slip value on the asperity is set to the excess over the surrounding non-asperity area for the preservation of the total moment.

The ground motions of the 1923 event were synthesized at several evaluation points by the proposed method named the superposition method. Two other simulating methods named the conventional method and the proportion method are also performed for comparison. At all the evaluation points the peak acceleration values obtained by the superposition method are obviously higher than those by other two methods, if the range of the error bar is taken into consideration. The superposition method results in the formulation of "the barrier model" in a frame of the semi-empirical simulation, and provides the upper limit of the high-frequency seismic radiation for the roughly estimated source model.

REFERENCES

- Aki, K. (1967), "Scaling Law of Seismic Spectrum", *J. Geophys. Res.*, 72, pp1217-1231.
- Ando, M. (1974), "Seismotectonics of the 1923 Kanto earthquake", *J. Phys. Earth*, 22, pp263-277.
- Bernard, P. and R. Madariaga (1984), "High-frequency seismic radiation from a buried circular fault", *Geophys. J. Roy. Astr. Soc.*, 78, pp1-17.
- Boore, D. M. (1983), "Stochastic simulation of high frequency ground motion based on seismological models of radiated spectra", *Bull. Seism. Soc. Am.*, 73, pp1865-1894.
- Boore, D. M. and J. Boatwright (1984), "Average Body-Wave Radiation Coefficients", *Bull. Seism. Soc. Am.*, 74, pp1615-1621.
- Brune, J. (1970), "Tectonic stress and the spectra of seismic shear waves from earthquakes", *J. Geophys. Res.*, 75, pp4997-5009.
- Brune, J. (1971), "Correction", *J. Geophys. Res.*, 76, pp5002.
- Dan, K. and T. Sato (1999), "A semi-empirical method for simulating strong ground motions based on variable-slip rupture models for large earthquakes", *Bull. Seism. Soc. Am.*, 89, pp36-53.
- Das, S. and K. Aki (1977), "Fault plane with barriers: a versatile earthquake model", *J. Geophys. Res.*, 82, pp5658-5670.
- Hartzell, S. H. (1978), "Earthquake aftershocks as Green's functions", *Geophys. Res. Lett.*, 5, pp1-4.
- Irikura, K. (1986), "Prediction of strong acceleration motions using empirical Green's function", *Proc. 7th Japan Conf. Earthquake Engineering*, pp151-156.
- Kamae, K., K. Irikura and A. Pitarka (1998), "A technique for simulating strong ground motion using hybrid Green's function", *Bull. Seism. Soc. Am.*, 88, pp357-367.
- Kamae, K. and K. Irikura (1998), "Source model of the 1995 Hyogo-ken Nanbu earthquake and simulation of near-source ground motion", *Bull. Seism. Soc. Am.*, 88, pp400-412.
- Kanamori, H. (1971), "Faulting of the great Kanto earthquake of 1923 as revealed by seismological data", *Bull. Earthquake Res. Inst. Tokyo Univ.*, 49, pp13-18.
- Liu, H. L. and D. V. Helmberger (1985), "The 23: 19 aftershocks of the 15 October 1979 Imperial Valley earthquake: More evidence for an asperity", *Bull. Seism. Soc. Am.*, 75, pp689-708.
- Madariaga, R. (1976), "Dynamics of an Expanding Circular Fault", *Bull. Seism. Soc. Am.*, 66, pp639-666.
- Matsu'ura, M., T. Iwasaki, Y. Suzuki and R. Sato (1980), "Static and dynamical study on the faulting mechanism of the 1923 Kanto earthquake", *J. Phys. Earth*, 28, pp119-143.
- Matsu'ura, M. and T. Iwasaki (1983), "Study on the coseismic and postseismic crustal movements associated with the 1923 Kanto earthquake", *Tectonophysics*, 97, pp201-215.
- Sato, H. (1990), "Unified approach to amplitude attenuation and coda excitation in the randomly inhomogeneous lithosphere", *Pure Appl. Geophys.*, 132, pp93-121.
- Sato, T., D. V. Helmberger, P. G. Somerville, R. W. Graves and C. K. Saikia (1998), "Estimates of regional and local strong motions during the great 1923 Kanto, Japan earthquake (Ms 8.2). Part 2: Forward simulation of seismograms using variable-slip rupture models and estimation of near-fault long-period ground motions", *Bull. Seism. Soc. Am.*, 88, pp206-227.
- Sato, T. and T. Hirasawa (1973), "Body wave spectra from propagating shear cracks", *J. Phys. Earth*, 23, pp323-331.
- Wald, D. J. and P. Somerville (1995), "Variable-Slip Model of the Great 1923 Kanto, Japan, Earthquake: Geodetic and Body-Waveform Analysis", *Bull. Seism. Soc. Amer.*, 85, pp159-177.